Electronic Supplementary Material (ESI) for ChemComm.

Supplementary Information

Probing nanomechanical interactions of SARS-CoV-2 variants Omicron and XBB with common surfaces

Yuelong Xiao, Bin Zheng, Xuan Ding and Peng Zheng*

State Key Laboratory of Coordination Chemistry, Chemistry and Biomedicine Innovation Center (ChemBIC), School of Chemistry and Chemical Engineering, Nanjing University, Nanjing, Jiangsu, 210023, China

*Corresponding author: Correspondence and requests for materials should be addressed to P.Z. (Email: pengz@nju.edu.cn)

This Supplementary Information Includes:

Supplementary Methods

Protein engineering. The genes were ordered from GenScript Inc. The RBD construct contains the SARS-CoV-2 spike protein (residues 319–536), followed by a GGGGS linker and an 8XHis tag in a pcDNA3.4 vector. A C-terminal NGL was added to the RBD for use in the AFM-SMFS experiment. OaAEP1(C247A) is a cysteine 247 to alanine mutant of asparaginyl endoprotease 1 from *Oldenlandia affinis*, abbreviated as OaAEP1 here. The expression and purification of OaAEP1 are according to this reference[1]. ELP is an elastin-like polypeptide[2]. RBD proteins were expressed in Expi293 cells with OPM-293 CD05 serum-free medium. For protein purification of RBD with 8XHis-tag, the culture supernatant was passed through a Ni-NTA affinity column. Proteins were further purified by gel filtration. Protein concentrations were routinely determined by Nanodrop 2000.

Protein immobilization. The AFM probes (MLCT-BIO-DC, Bruker Corp.) were used for our surface modification through the method we proposed previously. In brief, to add the NH_2 group firstly, probes were cleaned by plasma and immersed in 2% (v/v) APTES toluene solution for 1 h. Then NH_2-functionalized probes were reacted with a solution mixture of 2 mM $ImSO_2N_3$, 4 mM K_2CO_3, and 20 M $CuSO_4$ to change the amino group into the N_3 group. After flushing, they were further immersed in hetero-crosslinker DBCO-PEG_4-maleimide (4 mM in DMSO) at 37 °C for 1 h to add the maleimide group. Finally, the peptide C-ELP_{20}-NGL was reacted onto the surface of probes. Probes were cleaned with water and can be stored at 4 °C for weeks. For AFM-SMFS measurement, probes were incubated with 60 μL storage buffer containing 60 μM RBD-NGL and 3 μM OaAEP1 for 30 min.

Surface preparation. In this experiment, three different surfaces (paper, plastic, and gold) were prepared, which are ubiquitous in daily life and have drawn much attention. Cellulose film was selected as a substitute for the paper surface, which remained intact in the AFM-SMFS buffer throughout the experimental process. The plastic surface was made of polystyrene material and cleaned by washing with Milli-Q water and ethanol, followed by drying with high-purity nitrogen. The gold-coated silicon wafers were first sonicated in isopropanol and Ethanol for 10 min, then flushed with Milli-Q water and Ethanol. The gold wafer shards were dried using high-purity nitrogen and subjected to plasma treatment to eliminate any remaining residues. All the surface samples were immediately used for the AFM-SMFS measurements after the cleaning procedure.

AFM-SMFS experiment. Single-molecule AFM experiments were performed with the commercial JPK ForceRobot AFM. The D tip of the cantilever was used to probe the interaction between the RBD and three different surfaces. The Si_3N_4 cantilevers were functionalized and immobilized with target proteins covalently as described above. After calibration, Its accurate spring constant was determined by a thermally induced fluctuation method. The probe was contacted with the surfaces for a brief period (~50 ms) at 300 pN, then the probe retracted under a constant velocity of 800 nm/s. As a

result, a force-extension curve, possibly including the interaction event, was obtained. Spring constants of cantilevers (k) in AFM-SMFS experiments are shown as follows:
$k_{WT\text{-}1}$ = 27.1 pN/nm, $k_{BA.1\text{-}1}$ = 27.7 pN/nm, $k_{XBB\text{-}1}$ = 28.6 pN/nm
$k_{WT\text{-}2}$ = 29.3 pN/nm, $k_{BA.1\text{-}2}$ = 31.3 pN/nm, $k_{XBB\text{-}2}$ = 30.4 pN/nm
$k_{WT\text{-}3}$ = 30.0 pN/nm, $k_{BA.1\text{-}3}$ = 28.9 pN/nm, $k_{XBB\text{-}3}$ = 27.4 pN/nm

SMFS data analysis. The data were first filtered by JPK data processing and then analyzed by Igor Pro 6.12. The worm-like chain model (Eq. 1) was used to fit curves with a persistence length of ~0.4 nm.

$$F(x) = \frac{k_B T}{p}\left[\frac{1}{4}\left(1 - \frac{x}{L_c}\right)^{-2} - \frac{1}{4} + \frac{x}{L_c}\right] \quad (1)$$

where *F(x)* is the force applied to the polymer (polypeptide chain) under a polymer extension *x*. *p* is the persistence length of the polymer. L_c is the contour length. k_B is the Boltzmann constant, and *T* is the temperature in kelvin.
Gaussian function (Eq. 2) was used to fit the histogram.

$$f(x) = W_0 + W_1 * e^{-\left(\frac{x - w_2}{w_3}\right)^2} \quad (2)$$

where W_0, W_1, W_2 and W_3 are arbitrary real constants ($W_3 \neq 0$).

Supplementary Note

Protein sequence of GL-**(ELP)$_{20}$**-Cys (MW: ~10 kDa):
MGLHHHHHHGS**VPGEGVPGVGVPGVGVPGVGVPGVGVPGAGVPGAGVP**
GGGVPGGGVPGEGVPGEGVPGVGVPGVGVPGVGVPGVGVPGAGVPGA
GVPGGGVPGGGVPGEGRSC

Protein sequence of **RBD (WT, 319-536,** MW: ~26 kDa**)**
RVQPTESIVRFPNITNLCPFGEVFNATRFASVYAWNRKRISNCVADYSVLY
NSASFSTFKCYGVSPTKLNDLCFTNVYADSFVIRGDEVRQIAPGQTGKIAD
YNYKLPDDFTGCVIAWNSNNLDSKVGGNYNYLYRLFRKSNLKPFERDIST
EIYQAGSTPCNGVEGFNCYFPLQSYGFQPTNGVGYQPYRVVVLSFELLHA
PATVCGPKKSTNLVKNGGGGSHHHHHHHHNGL

Protein sequence of **RBD (Omicron, 319-536,** MW: ~26 kDa**)**
RVQPTESIVRFPNITNLCPFDEVFNATRFASVYAWNRKRISNCVADYSVLY
NLAPFFTFKCYGVSPTKLNDLCFTNVYADSFVIRGDEVRQIAPGQTGNIA
DYNYKLPDDFTGCVIAWNSNKLDSKVSGNYNYLYRLFRKSNLKPFERDIS
TEIYQAGNKPCNGVAGFNCYFPLRSYSFRPTYGVGHQPYRVVVLSFELLH
APATVCGPKKSTNLVKNGGGGSHHHHHHHHNGL

Protein sequence of **RBD (XBB, 319-536,** MW: ~26 kDa**)**
RVQPTESIVRFPNITNLCPFHEVFNATTFASVYAWNRKRISNCVADYSVIY
NFAPFFAFKCYGVSPTKLNDLCFTNVYADSFVIRGNEVSQIAPGQTGNIAD
YNYKLPDDFTGCVIAWNSNKLDSKPSGNYNYLYRLFRKSKLKPFERDIST
EIYQAGNKPCNGVAGSNCYSPLQSYGFRPTYGVGHQPYRVVVLSFELLH
APATVCGPKKSTNLVKNGGGGSHHHHHHHHNGL

Supplementary Figures

```
WT    319 RVQPTESIVRFPNITNLCPFGEVFNATRFASVYAWNRKRISNCVADYSVLYNSASFSTFKCYGVSPTKLNDL 390
BA.1  319 RVQPTESIVRFPNITNLCPFDEVFNATRFASVYAWNRKRISNCVADYSVLYNLAPFFTFKCYGVSPTKLNDL 390
XBB   319 RVQPTESIVRFPNITNLCPFHEVFNATTFASVYAWNRKRISNCVADYSVIYNFAPFFAFKCYGVSPTKLNDL 390

WT    391 CFTNVYADSFVIRGDEVRQIAPGQTGKIADYNYKLPDDFTGCVIAWNSNNLDSKVGGNYNYLYRLFRKSNLK 462
BA.1  391 CFTNVYADSFVIRGDEVRQIAPGQTGNIADYNYKLPDDFTGCVIAWNSNKLDSKVSGNYNYLYRLFRKSNLK 462
XBB   391 CFTNVYADSFVIRGNEVSQIAPGQTGNIADYNYKLPDDFTGCVIAWNSNKLDSKPSGNYNYLYRLFRKSKLK 462

WT    463 PFERDISTEIYQAGSTPCNGVEGFNCYFPLQSYGFQPTNGVGYQPYRVVVLSFELLHAPATVCGPKKSTNLVKN 536
BA.1  463 PFERDISTEIYQAGNKPCNGVAGFNCYFPLRSYSFRPTYGVGHQPYRVVVLSFELLHAPATVCGPKKSTNLVKN 536
XBB   463 PFERDISTEIYQAGNKPCNGVAGSNCYSPLQSYGFRPTYGVGHQPYRVVVLSFELLHAPATVCGPKKSTNLVKN 536
```

Fig. S1 Multiple sequence alignment of the variants BA.1 and XBB with the wild type RBD (319-536).

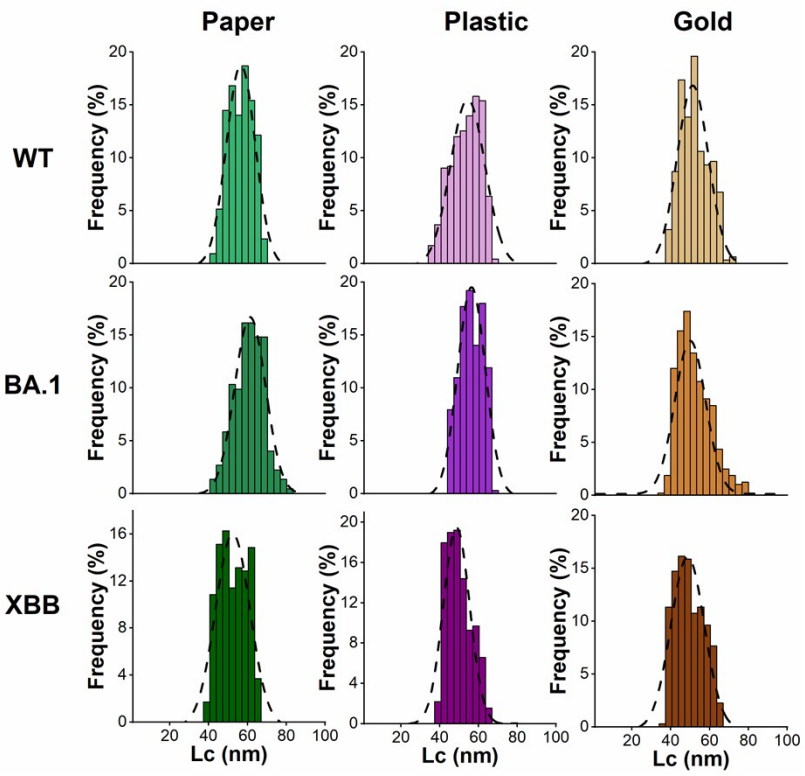

Fig. S2 The histogram of Lc is shown.

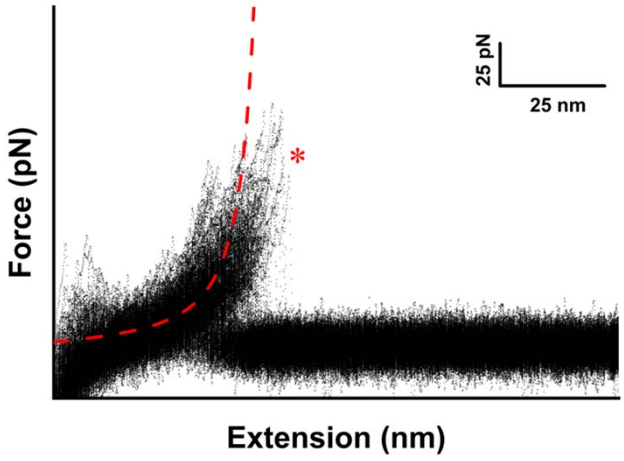

Fig. S3 Superimposition of unbinding curves (density plot) of the unbinding of RBD from the surface.

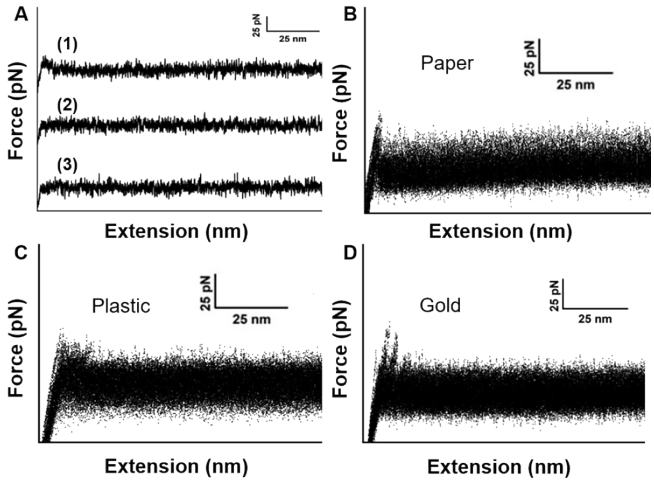

Fig. S4 Negative control experiment using AFM-tip without RBD coating. (A) Representative force-extension curves show no specific binding event between the tip without the RBD and the surfaces. (B-D) Superimposition of unbinding curves (density plot).

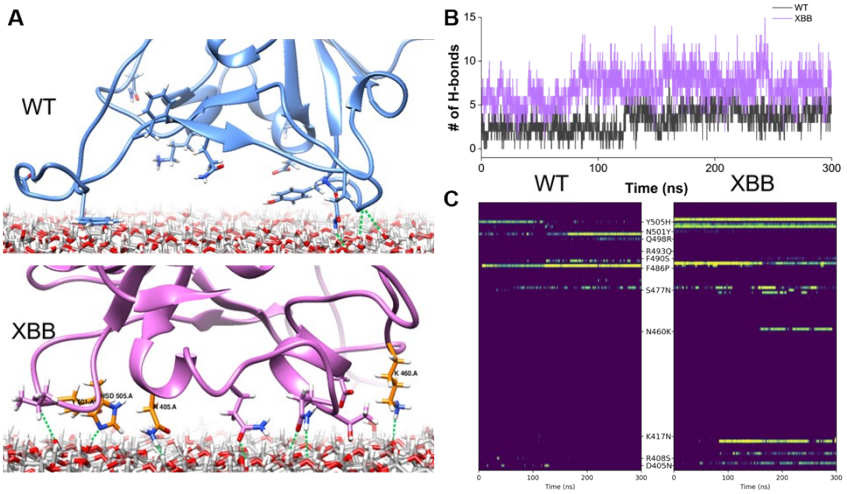

Fig. S5 MD simulation results for interaction between RBD and paper (cellulose) surface. (A) The enlarged structure shows the hydrogen bonds (dashed line). H-bonds are colored green. (B) MD simulations show the number of hydrogen bonds formed between RBD and paper (cellulose) surface (C) The evolution of the number of hydrogen bonds for each mutation involved during MD simulations.

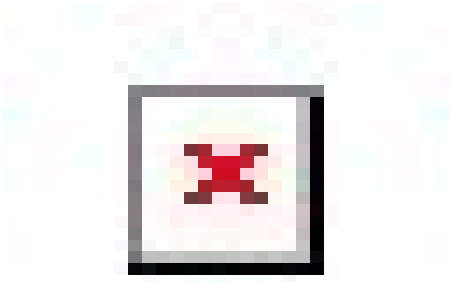

Fig. S6 Diagram illustrating the unbinding force and significance difference.

Supplementary Tables

Table S1. The statistical analysis of Lc.

	Paper (nm)	Plastic (nm)	Gold (nm)
WT	56.5 ± 0.4	54.4 ± 0.6	51.0 ± 0.6
Omicron	61.3 ± 0.4	56.3 ± 0.4	50.0 ± 0.6
XBB	52.3 ± 0.7	48.6 ± 0.5	48.7 ± 0.6

Table S2. The ratios of adhesion forces for RBD mutants compared to the wild-type.

	Paper (%)	Plastic (%)	Gold (%)
(Omicron-WT)/WT	28	9	4
(XBB-WT)/WT	17	7	27

Supplementary References：

1. R. Yang, Y. H. Wong, G. K. T. Nguyen, J. P. Tam, J. Lescar and B. Wu, *J. Am. Chem. Soc,* 2017, **139**, 5351-5358.
2. W. Ott, M. A. Jobst, M. S. Bauer, E. Durner, L. F. Milles, M. A. Nash and H. E. Gaub, *ACS Nano,* 2017, **11**, 6346-6354.